ELSEVIER

Journal of Molecular Catalysis A: Chemical 165 (2001) 45–54

JOURNAL OF MOLECULAR CATALYSIS A: CHEMICAL

www.elsevier.com/locate/molcata

Application of the impulse oscillation model for modelling the formation of peroxocarbonates via carbon dioxide reaction with dioxygen transition metal complexes
A comparison with the experimental results obtained for $Rh(\eta^2\text{-}O_2)ClP_3$ [P = phosphane ligand]

Marek A. Borowiak [a,*], Michal H. Jamróz [a], Jan Cz. Dobrowolski [a], Krzysztof Bajdor [a], Jan K. Kazimirski [a], Joelle Mascetti [b], Eugenio Quaranta [c], Immacolata Tommasi [c], Michele Aresta [c]

[a] *Industrial Chemistry Research Institute, Rydygiera 8, 01-793 Warsaw, Poland*
[b] *Laboratoire de Spectroscopie Moleculaire et Crystalline, U.R.A. 124 CNRS, 351 Cours de Liberation, 33405 Talence, France*
[c] *Dipartimento di Chimica, Università di Bari, Campus Universitario, 70126 Bari, Italy*

Received 10 July 2000; accepted 11 September 2000

Abstract

The reaction of CO_2 with (η^2-dioxygen)-transition metal complexes to give peroxocarbonates has been modelled using the Impulse Oscillation Model (IOM).[1] In accordance with our experimental findings concerning the reactivity of $P_3ClRh(\eta^2\text{-}O_2)$ (P = phosphane ligand) complexes towards carbon dioxide, application of the model to this reaction shows that the insertion of carbon dioxide into the O–O bond is the preferred pathway. In fact, the probability for CO_2 insertion into the O–O bond equals maximum to 0.98 while into the M–O bond equals to 0.02. The concordance of calculated and experimental stretching frequencies indicates the possibility of identifying, through the vibration modes, proper ligands and metal systems that behave as selective catalysts at molecular level.

Keywords: Impulse oscillation model (IOM); Carbon dioxide; Dioxygen complexes; Rhodium-complexes; Peroxocarbonato-complexes

*Corresponding author. Tel.: +48-22-633-9794;
fax: +48-22-639-8608.
E-mail address: mabor@aquila.ichp.waw.pl (M.A. Borowiak).

[1] Supporting Information Available — IOM model (block diagram, background and description of IOM); moment of "first appearance" of the reactivity impulse for the reactant and the catalyst; time of synchronization of the reactivity impulses and set of equations for the four cases (1–4), the two pathways (path A and B) and the eight phase combinations considered in the paper; S_A values for $Rh(^{18}O_2)$ labelled moiety for different modes and combination of phases for the four initial cases; S_A values for labelled $C^{18}O_2$ for different modes and combination of phases for the four initial cases; effect of isotopic labelling; IOM package-set of tools.

1381-1169/01/$ – see front matter
PII: S1381-1169(00)00428-3

1. Introduction

Carbon dioxide has been used as modulator of the dioxygen oxidative properties towards olefins, using Rh(I) catalysts that, in the same operative conditions, can promote the synthesis of cyclic organic carbonates [1,2]. Peroxocarbonates, LnXRhOOC(O)O, are likely to be intermediates in both the olefin oxidation and carbonate formation reactions [1,2]. Recently, the mechanism of formation of Rh(III)-peroxocarbonates from CO_2 and $P_3ClRh(\eta^2\text{-}O_2)$ (P = phosphane) complexes has been investigated to ascertain if the heterocumulene inserts into the O–O (path A, Scheme 1) or the Rh–O bond (path B, Scheme 1) of the $Rh(\eta^2\text{-}O_2)$ moiety [3]. We have demonstrated that formation of peroxocarbonate occurs via insertion of CO_2 into the O–O bond of the O_2 molecule η^2-coordinated to Rh (path A, Scheme 1). In this paper, we present the results of a theoretical study using the "Impulse Oscillation Model, IOM" [4–11] applied to the general case of the reaction of a hexacoordinated dioxygen metal complex with CO_2. IOM gives an indication about the possible reaction pathways (paths A and B, Scheme 1) and allows to select metal systems that behave according to the proposed reaction mechanism.

IOM treats the reacting molecules as a set of their vibrational modes and states that, if the necessary spatial and energy conditions are fulfilled, the requirement for a reaction may occur is the synchronization of the appropriate charge distribution in the reactant molecules (i.e. substrate and catalytic centre) during the vibration. The favourable distribution of charges on the reactant and the catalytic centre is referred as the "reactivity impulse". The charge distribution can be related to momentary bond-length in the different vibration stages. However, IOM uses only three particular partial charge-distributions corresponding to the equilibrium length (stage 0.5), the minimum (stage 0) or maximum (stage 1) amplitude of the vibrator.

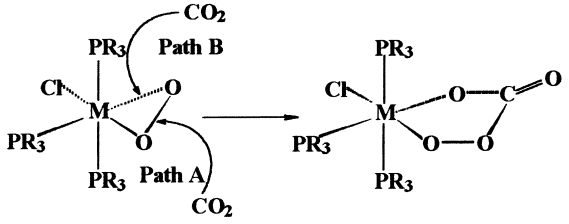

Scheme 1. Reaction pathways for peroxocarbonate formation.

To model a reaction by IOM, the time of first appearance of the reactivity impulse for the assembled system "reactant-catalytic center" must be calculated together with the time of synchronization of the impulses, that in IOM model represents the time for the reaction to occur.

Per each vibrator considered in the model, an appropriate range of frequencies is assumed. It may be wide enough to include a variety of metal systems (metal plus ligands), that are potential catalysts for the reaction under consideration. As a next, the synchronization condition is tested for all combinations of the ranges of all vibrators.

The results of IOM calculations are a narrow set of vibration frequencies for which the synchronization condition is fulfilled and the probability that the reaction occurs according to a given pathway.

Calculations for IOM are performed using IOMO software [12] for PC. The outcome is a set of wavenumber ranges specific per each reaction pathway. These data are the input for the IOMAB software [2] that determines the selectivity towards each of the possible reaction paths (A or B), each corresponding to a well defined reaction mechanism.

2. The conditions used in IOM

In this work, the condition of synchronization for either path A or B in Scheme 1 has been calculated. Four different initial cases (i.e. for $t = 0$) have been considered (Scheme 2). [3] The stages at $t = 0$ for the four cases reported above are given in Table 1.

[2] IOMAB is the software for the selection of path A and B. See also [12]. The selectivity towards path A (probability of path A), S_A, is calculated using the following formula: $S_A = (A + AB + BA)100/[A + B + 2(AB + BA)]$ where: A, B, AB, BA represent the wavenumbers that make the synchronization possible.

[3] *Case 1*: Full symmetric metal complex and symmetric linear CO_2. *Case 2*: Full symmetric metal complex and symmetric non-linear carbon dioxide. *Case 3*: Geometry of the complex corresponding to the reactivity impulse for path B and symmetric non-linear carbon dioxide. *Case 4*: Geometry of the complex corresponding to the reactivity impulse for path A and symmetric non-linear CO_2. The term "full symmetric metal complex" refers to a non-deformed geometry of the M–O_2 moiety, with all bonds at the equilibrium length. The symmetric CO_2 molecule has the two C–O bonds equivalent, either in the linear or bent configuration.

Table 1
Definition of the stages at $t = 0$ for the four different cases considered in Scheme 2

Mode	Description	Case of $t = 0$			
		1	2	3	4
$\nu 1$	O–O stretching	0.5	0.5	0	1
$\nu 2$	O–M–O asymmetric stretching	0.5;0.5[a]	0.5;0.5[a]	0;1[a]	0.5;0.5[a]
$\nu 3$	O–M–O symmetric sretching	0.5	0.5	1	0
$\nu 4$	M(O–O) bending[b]	0	0	1	0
$\nu 5$	M–P stretching	0.5	0.5	1	0
$\nu 6$	P–M–P bending[b]	0	0	1	0
$\nu 7$	M–Cl stretching	0.5	0.5	1	0
$\nu 8$	O–C–O asymmetric stretching	0.5;0.5[a]	0.5;0.5[a]	0.5;0.5[a]	0.5;0.5[a]
$\nu 9$	O–C–O symmetric Stretching	0.5	0.5	0.5	0.5
$\nu 10$	O–C–O bending	0	1	1	1

[a] The pair of stages (0.5;0.5 or 0;1) corresponding to the pair of bonds in the moiety.
[b] The stage 0 means the equilibrium angle in the moiety (in plane), the stage 1 — the maximum angle (out of plane).

We have selected for the calculations 10 key vibration modes, seven characteristic of the metal system and three of CO_2 (Table 1). In this way, it is possible to determine how the ancillary ligands and the metal itself modulate the reactivity of the system.

For the definition of the reactivity impulses for path A and B, it has been assumed that the choice at the molecular level is driven by the synchronization of the reactivity impulse of carbon dioxide with all possible reactivity impulses of the metal dioxygen-complex. Therefore, the impulses for path A and B should differ for the partial charge on the metal and the geometry of the M–O_2 system (O–O and M–O bonds). Consequently, it has been assumed that for path A, in which the O–O bond should be cleaved, the best momentary state for the reaction is given by the symmetric (same length of both M–O bonds) minimum overlapping of the O–O bonding orbitals and minimum of charge separation at the metal centre. Conversely, path B requires the maximum overlapping of the O–O bonding orbitals, asymmetry of the M–O bonds (that must be different in length) and maximum of charge separation at the metal center. For both paths, the same impulse for the CO_2 molecule has been assumed, corresponding to a bent molecule (angle close to 133°) with two quite different C–O bonds. [4] The resulting characters of the reactivity impulses are listed in Table 2.

It must be noted that during one full vibration, the equilibrium length of any bond (designed as the momentary state 0.5) occurs twice, i.e. during the elongation (this phase is indicated as R) and the contraction (phase K). This fact is relevant to the determination of the first appearance of the reactivity impulse. In this application of IOM, state 0.5 (equilibrium distance for the bonds) at time $t = 0$ is assumed for five stretching

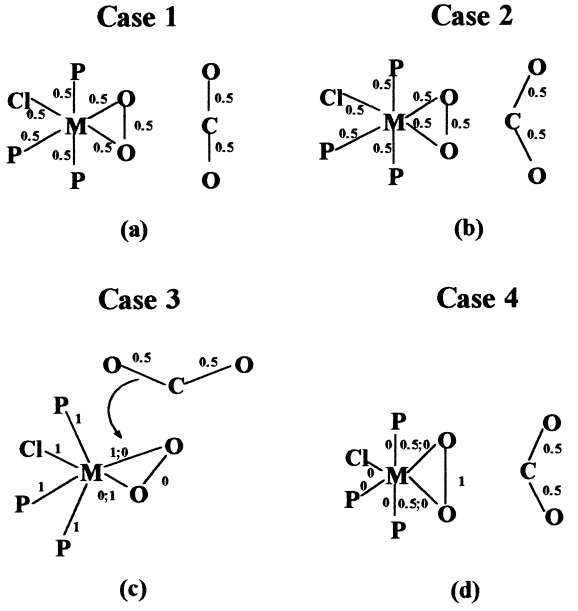

Scheme 2. The four different initial cases considered ($t = 0$).

[4] As CO_2 approaches the metal centre, the deviation from the linear configuration will increase progressively up to reach a OCO angle of ca. 133° [13,14].

Table 2
Characters of "reactivity impulses" according to path A or B (see Scheme 1)

Mode	Impulse for path A	Impulse for path B
ν1; O–O stretching	1	0
ν2; O–M–O asymmetric stretching	0.5;0.5	0;1
ν3; O–M–O symmetric stretching	0	1
ν4; M(O–O) bending	0	1
ν5; M–P stretching	0	1
ν6; P–M–P bending	0	1
ν7; M–Cl stretching	0	1
ν8; O–C–O asymmetric stretching	0;1	0;1
ν9; O–C–O symmetric stretching	1	1
ν10; O–C–O bending	1	1

symmetric modes (ν1, ν3, ν5, ν7, ν9; Table 1) and for two asymmetric stretching modes, ν2 and ν8. In each case, both R and K phases are considered.

The combination of the two phases for all seven modes gives 128 different situations. To simplify the description, the same phase for each symmetric stretching mode is combined with both phases of the asymmetric stretching modes, giving rise to only eight combinations. A combination indicated as RKR means that five stretching modes (ν1, ν3, ν5, ν7, ν9) are in the elongation phase (R), ν2 mode is in the contraction phase (K) and ν8 is in the elongation phase (R). The full IOM model (see supporting information) for the 10 considered modes (Table 2) contains 44 sets of 10 equations. The number of sets results from four different cases of definition of $t = 0$, the two reaction paths and eight phase combinations. It is reduced from 64 to 44 due to the fact that identical equations are found for some particular situations. For each set of 10 equations, calculations are made using three different ranges of wavenumbers corresponding to: (1) M–$^{16}O_2$ and $^{12}C^{16}O_2$; (2) M–$^{18}O_2$ and $^{12}C^{16}O_2$, and (3) M–$^{16}O_2$ and $^{12}C^{18}O_2$. The ranges of frequency values used in the calculations are reported in Table 3.

3. Results and discussion

The outcome of the calculations per each of the four cases 1–4 reported above are discussed, for the phase combination at $t = 0$, for both the ^{16}O and ^{18}O species. Data are discussed in terms of S_A — selectivity towards path A (Scheme 1).

Fig. 1 shows for each case 1–4, for non labelled reactants, the S_A values for different combinations of modes and phases and the averaged selectivity.

3.1. Case 1

The symmetric linear CO_2 molecule (a very unlike reactive state) is assumed to meet the dioxygen-complex in its full symmetric conformation. Also in these conditions, S_A is lower than 50% ($S_B > 50\%$) only in 23 out of the 80 considered cases (8 phase combinations and 10 equations). This is particularly true for the RRK combination: the selectivity for path A is lower than 50% for all the modes.

It is interesting to note that the vibration that should mostly favour the M–O cleavage (i.e. ν2) gives a selectivity for path B that is only 51% for the RRK phase

Table 3
Ranges of frequencies (cm^{-1}) used in the calculations

Mode	^{16}O	M($^{18}O_2$)	$C^{18}O_2$
ν1; O–O stretching	850–900	801–831	850–900
ν2; O–M–O asymmetric stretching	530–570	511–531	530–570
ν3; O–M–O symmetric stretching	400–500	400–500	400–500
ν4; M(O–O) bending	200–250	200–250	200–250
ν5; M–P stretching	370–399	370–399	370–399
ν6; P–M–P bending	150–200	150–200	150–200
ν7; M–Cl stretching	285–325	285–325	285–325
ν8; O–C–O asymmetric stretching	2310–2350	2310–2350	2285–2310
ν9; O–C–O symmetric stretching	1240–1400	1240–1400	1240–1400
ν10; O–C–O bending	630–800	630–800	630–680

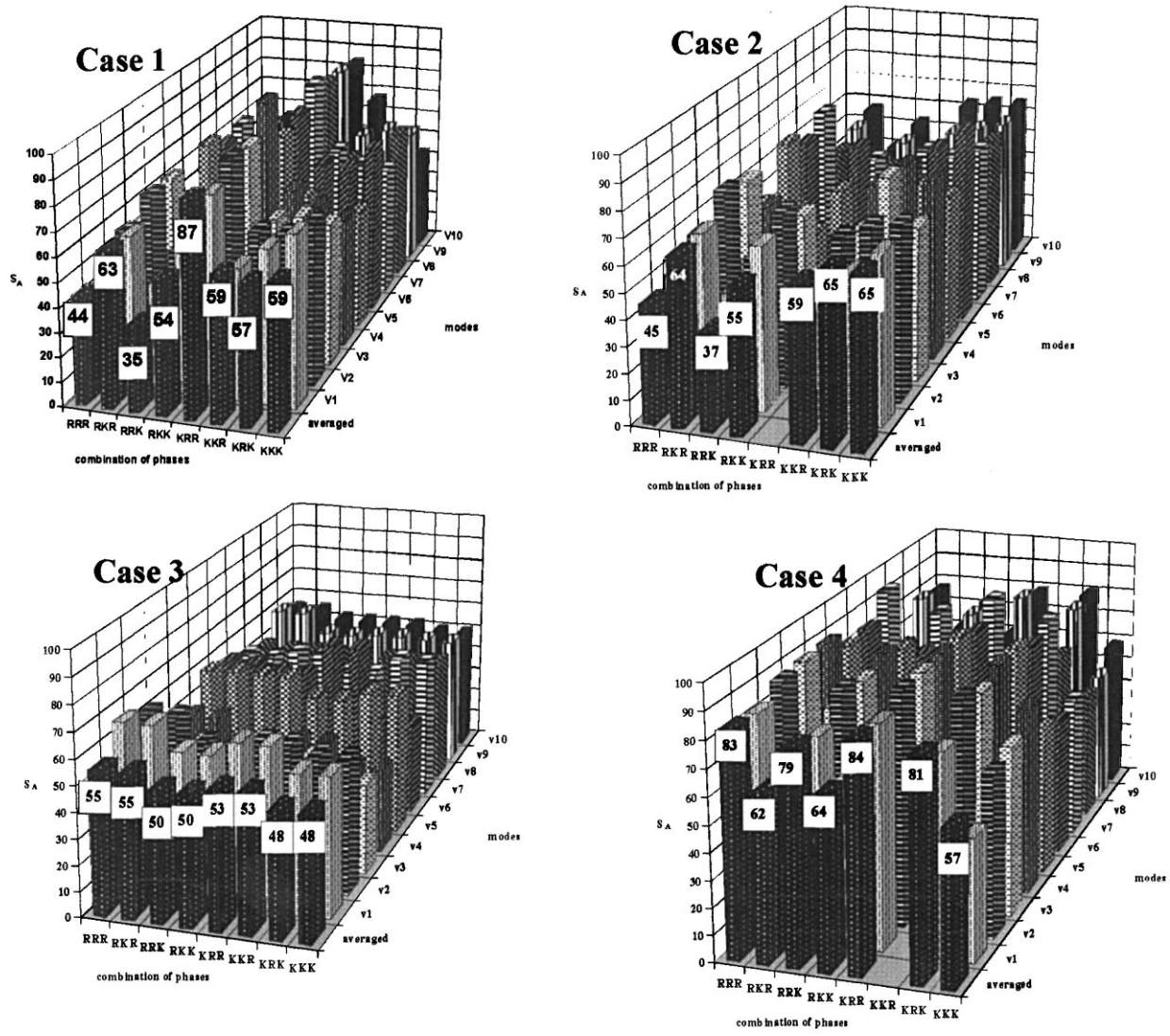

Fig. 1. Selectivity and averaged selectivity for path A (non labelled reactants) for different modes and combinations of phases for the four initial cases.

combination and 45% when the RRR phase occurs. In all other phase combinations, S_B is lower than 40%. When the ^{18}O species are considered, four combinations out of eight of the type RXX (X = R or K) prefer path B, if the $Rh^{18}O_2$ moiety is reacted with $C^{16}O_2$. Conversely, if $C^{18}O_2$ is reacted with $Rh^{16}O_2$, only the RRR combination prefers path B. Thus ^{18}O isotope labelling at CO_2, seems to reduce the probability of the M–O cleavage with respect to the O–O cleavage.

3.2. Case 2

Case 2 considers the bent CO_2 molecule: only 20 out of the 80 calculated values of S_A are lower than 50% (Fig. 1). This occurs with the RRR and RRK phase combination. The $\nu 2$ gives for S_B a value higher than 50% only for the RRK combination.

With ^{18}O species, the results are very similar to those observed in case 1. The KKK phase combination does

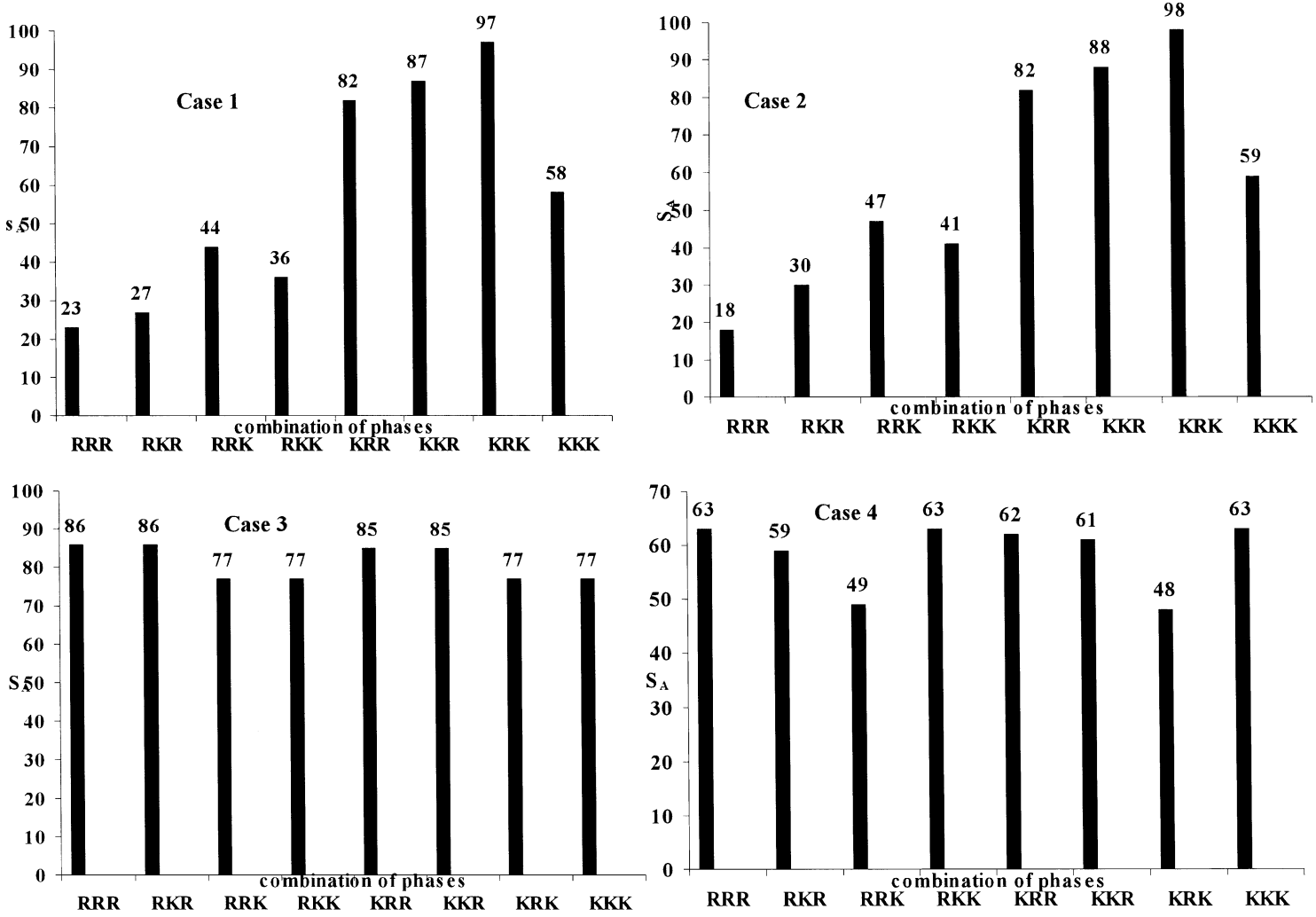

Fig. 2. Averaged selectivity for Rh($^{18}O_2$) labelled moiety for different combination of phases and cases.

not favour O–O splitting when $C^{18}O_2$ is reacted with M–$^{16}O_2$.

3.3. Case 3

One could expect that, with the M–O_2 moiety of the complex ready to react according to path B, S_B should be very high. Fig. 1 shows that also in this case the selectivity for path A is higher. Only for 18 of the 80 values S_B is higher than 50%. This finding illustrates that the readiness of only one component of the system to react according to a pathway, is not a condition sufficient for the reaction to occur according to that path.

Isotope labelling shows that when M–$^{18}O_2$ is reacted with $C^{16}O_2$, no one phase combination prefers path B (Fig. 2). S_A ranges for all phases between 60 and 70%. If $M^{16}O_2$ is reacted with $C^{18}O_2$, 54 out of the 80 calculated values show preference for path A.

3.4. Case 4

Case 4 presents the M–O_2 complex ready to react according to path A. As a matter of facts, only one S_A value is lower than 50% (Fig. 1) and the average selectivity is always higher than 50%.

Similarly, only one phase combination (RRK) does not prefer path A when $M^{18}O_2$ is reacted with $C^{16}O_2$ (Fig. 2) and only one out of 80 S_A values is lower than 50% when $M^{16}O_2$ is reacted with $C^{18}O_2$.

Fig. 3 shows the selectivity toward path A averaged over the four cases and the 10 modes for different sets of phases. For all of them the selectivity is higher than 50%.

Therefore, path A is by far the most favoured process, regardless of the initial case and phase combination.

Also when ^{18}O species are considered (Figs. 4 and 5), the large majority of cases indicates insertion of CO_2 into the O–O bond as the most like reaction mechanism. Only for the combination RRR, S_A is lower that 50% (48%) and only for the $Rh^{18}O_2$ metal system (Fig. 4). When the $C^{18}O_2$ species is assumed to react with Rh–$^{16}O_2$, the averaged selectivity for path A is always higher than 50% (Fig. 5).

The influence of isotopic labelling is shown by the value $^*S_A$ calculated according to the equation:

$$^*S_A = \frac{[S_A(^{16}O) - S_A(^{18}O)]100}{S_A(^{16}O)}$$

The modes most sensitive to isotopic labelling result to be ν7, ν6, ν2, ν5 and ν1 (see supporting information).

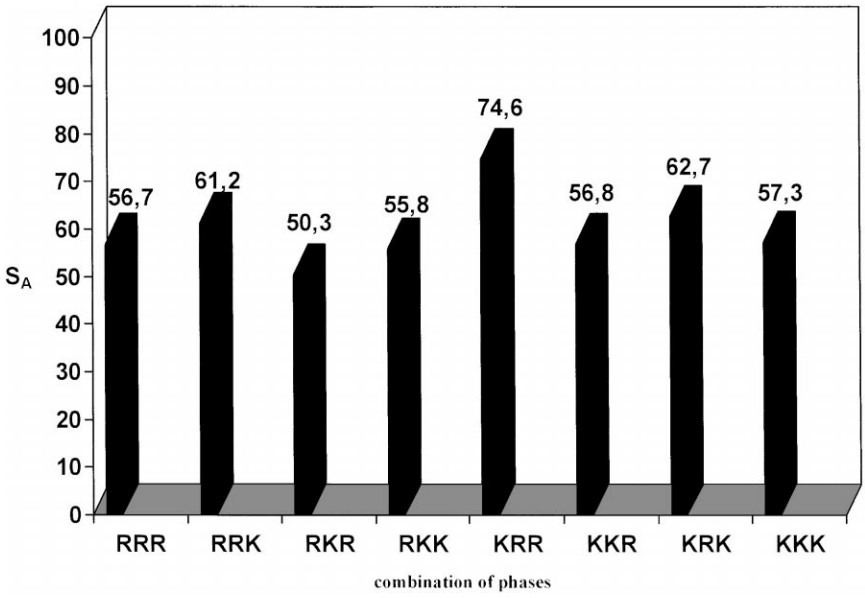

Fig. 3. Averaged selectivity for non-labelled reactants.

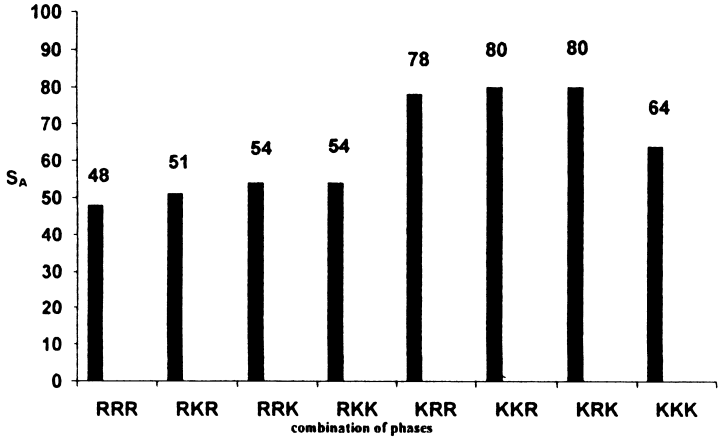

Fig. 4. Averaged selectivity for Rh($^{18}O_2$) labelled moiety.

Fig. 6 compares the selectivity for labelled and non labelled species.[5] The result of the application of the IOM to the reaction of an η^2-O_2 six-coordinated Rh complex with CO_2 clearly shows that the reaction takes place through the insertion of CO_2 into the O–O bond. In fact, the average probability for such CO_2 insertion is well over 50% in all possible cases considered and reaches a maximum of 98% (Fig. 6).[6]

Per each of the considered vibration modes of the peroxo-complex the ranges of frequencies, for which synchronization according to path A is found, have been calculated. The results are summarized in Table 4 and compared with the experimental results.

We report in the last column of Table 4 the IR frequencies experimentally found for the complex Rh-$(O_2)P_3Cl$ (P = PEt_2Ph) that reacts with CO_2 to afford the peroxocarbonate $Rh(CO_4)P_3Cl$ via CO_2 insertion into the O–O bond[7] [3]. It is interesting to note that all the observed (ν1–ν3, ν5, ν7) vibrations are within 2 cm^{-1} with the calculated values. The fact that both the theoretical and experimental results point at the CO_2 insertion into the O–O bond of the M–O_2 moiety validates the IOM approach as a potential tool for catalyst design and finding the best metal system (metal centre and ligands) for catalytic applications.

Further work is in progress in order to compare, in a more extended way, the results of theoretical calculations with spectroscopic data. This approach is now being extended to modelling the interaction of CO_2/O_2 mixtures with olefins, promoted by transition metal systems.

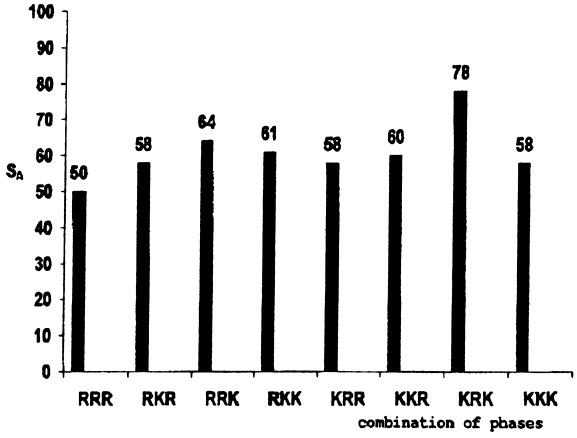

Fig. 5. Averaged selectivity for $C^{18}O_2$ labelled moiety.

[5] All other full representations for non labelled cases 1–4, and M–O_2 or CO_2 labelled systems are given as supporting informations and can be required to the editor.

[6] For a very limited number of selected ranges of vibrations the selectivity towards path B can be as high as 75% but confined to only very few of the 132 cases (footnote 4) (44 sets of 10 equations and three different isotope labelling at oxygen) considered.

[7] This pathway is preferred to the reaction with the M–O bond most probably because of the lower energy of the O–O bond (ca. 40 kcal mol^{-1}) with respect to the M–O bond (ca. 60 kcal mol^{-1}).

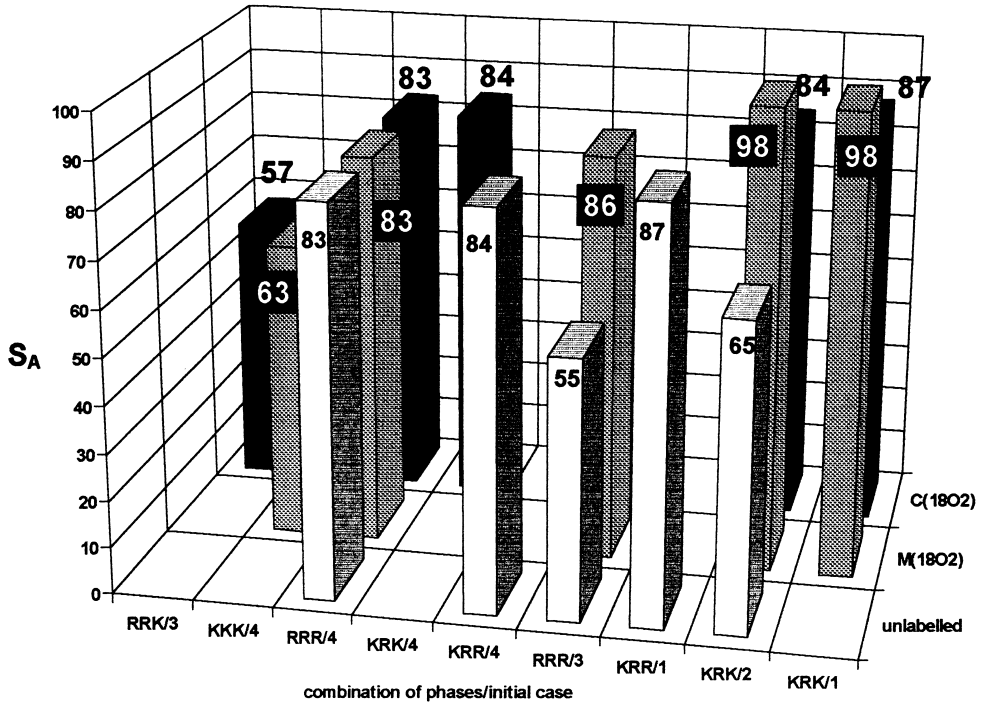

Fig. 6. Maximum selectivity.

Table 4
Ranges of calculated frequencies of the peroxo-complex agreeing with IOM synchronization for path A

Vibration mode	Calculated frequency ranges (cm^{-1})	Experimental IR absorptions (cm^{-1}) for $ClRh(O_2)(PEt_2Ph)_3$
ν1; O–O stretching	890;880;865;859	867
ν2; O–M–O asymmetric stretching	570;565;550;540	542
ν3; O–M–O symmetric stretching	498–492;479–474;453–450;439–432	446
ν4; M(O–O) bending	250;240;225;210	Not observed
ν5; M–P stretching	398–396;378–373;387–386	391
ν6; P–M–P bending	166–164	Not observed
ν7; M–Cl stretching	288–287;296–292;318–313	320

Acknowledgements

The finacial support by COST, project D3/007/94, is gratefully acknowledged. Polish authors thank KBN for financial support of the COST project by grant no. 3T0B03309. Italian authors wish to thank CNR (Contributo 98.01876.CT03) and MURST (Programme 40–60%) for financial support.

References

[1] M. Aresta, A. Ciccarese, E. Quaranta, C_1 Mol. Chem. 1 (1985) 267.
[2] M. Aresta, C. Fragale, E. Quaranta, I. Tommasi, J. Chem. Soc., Chem. Commun. (1992) 315.
[3] M. Aresta, C. Fragale, E. Quaranta, I. Tommasi, J. Mascetti, M. Tranquille, F. Galan, M. Fouassier, Inorg. Chem. 35 (1996) 4254.
[4] M.A. Borowiak, J. Mol. Catal. A: Chem. 156 (2000) 21.
[5] M.A. Borowiak, in: Proceedings of 196th American Chemical Society, National Meeting, Vol. 33(4), Los Angeles, USA, 1988, p. 647.
[6] M.A. Borowiak, Biophys. Chem. 32 (1988) 21.
[7] M.A. Borowiak, Introduction to Modelling of Catalytic System, Ossolineum, Wroclaw, Poland, 1990.
[8] M.A. Borowiak, Acta Pharm. Pol.-Drug Res. 48 (3/4) (1991) 75.
[9] M.A. Borowiak, Elementary Catalytic System Model for Rational Design of Catalysts at Atomic/Molecular Levels, Ossolineum, Wroclaw, Poland, 1991.
[10] M.A. Borowiak, J. Haber, J. Mol. Catal. 82 (1993) 327.
[11] M.H. Jamróz, M.A. Borowiak, Internet J. Chem. 1 (1998) 17, http://www.ijc.com/articles.
[12] M.A. Jamróz, M.A. Borowiak I.C.R.I. Internal report 1996.
[13] M. Aresta, E. Quaranta, I. Tommasi, New J. Chem. 18 (1994) 133.
[14] M. Aresta, E. Quaranta, I. Tommasi, P. Giannoccaro, A. Ciccarese Gazz. Chim. Ital. 125 (1995) 509.